iJRASET
International Journal For Research in
Applied Science and Engineering Technology

INTERNATIONAL JOURNAL FOR RESEARCH

IN APPLIED SCIENCE & ENGINEERING TECHNOLOGY

Volume: 8 Issue: VII Month of publication: July 2020

DOI: https://doi.org/10.22214/ijraset.2020.30411

International Journal for Research in Applied Science & Engineering Technology (IJRASET)
ISSN: 2321-9653; IC Value: 45.98; SJ Impact Factor: 7.429
Volume 8 Issue VII July 2020- Available at www.ijraset.com

To Predict the Bead Geometry Parameters and Shape Relationships in MIG Welding of Stainless Steel 301 by Mathematical Modelling

Aman Sehrawat[1], Dhruv Sharma[2], Artik[3], Pradeep Khanna[4]
[1, 2, 3]Student, MPA Engineering Division, NSUT, New Delhi
[4]Associate Professor, MPA Engineering Division, NSUT, New Delhi

Abstract: GMA Welding is a profoundly used technique in the joining industry. GMA Welding is used in automatic or semi-automatic modes depending upon the requirements. The versatility, portability, and lesser requirements for highly skilled labour to produce high quality welds makes it a better choice for joining purposes for small jobs as well as mass production. Due to the vast number of applications of the process, there is a need to construct a relationship between various user controlled parameters and the weld quality. In governing the mechanical properties of the weld, the weld bead plays a major role. Depending upon the values of the process parameters such as voltage, wire feed rate (WFR), torch angle, nozzle to plate distance(NPD) and welding speed, the geometrical properties of the weld bead such as width, penetration and weld reinforcement height are determined. The present investigatory work aims at developing a mathematical model to determine the weld bead geometry and shape parameters for stainless steel 301. A design matrix has been generated by the statistical methodology of Design of Experiments (DoE) to carry out experiments orderly. ANOVA technique has been used to check the adequacy of the results and graphically analysed using response surface methodology.
Keywords: GMA Welding, Weld Bead Geometry, Stainless Steel 301, ANOVA, Design of Experiments, RSM

I. INTRODUCTION

GMA Welding, being the preferred choice for choice for joining is widely used for industrial purposes. In GMA Welding, a constantly fed consumable wire spool is used which is used to build thick, high quality welds without any necessity of skilled labour. A welding gun feeds the wire with inert gas which shields the weld from atmospheric contamination. Solid-feed wire is used due to which there is minimum chances of any inclusion of slag due to the presence of flux. This also eradicates the need for any post-weld cleaning.

Bead geometry determines the mechanical strength of the weld. Appropriate fusion is required between base and the filler metal being deposited from the electrode to make good quality welds. The parent metal needs to be meticulously melted in order to have sufficient depth of the bead. [1] The schematic diagram of Weld Bead Geometry is shown in Fig 1.

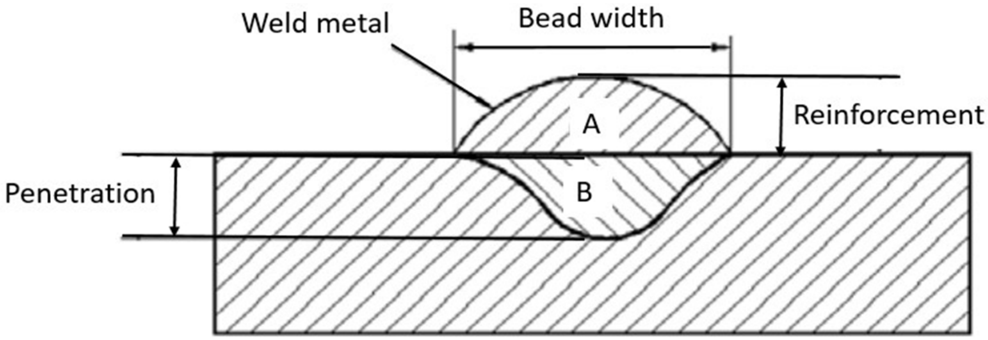

Fig. 1 : Schematic Diagram of Bead Geometry

For the purpose of effectual usage of automated welding systems, procedures and parameters are needed to be selected accordingly so as to ensure an adequate weld bead. [2] The process parameters selected to determine the weld bead are Wire Feed Rate, Voltage, Welding Speed, Torch Angle and Nozzle To Plate Distance. In recent practices, computerized techniques have increased the efficiency due to statistically devised experimentation. [3] Varying different values of the process parameters, weld bead properties (Width, Penetration, Reinforcement height, WRFF, WPSF) are analysed to determine the values for obtaining the optimum bead.

International Journal for Research in Applied Science & Engineering Technology (IJRASET)
ISSN: 2321-9653; IC Value: 45.98; SJ Impact Factor: 7.429
Volume 8 Issue VII July 2020- Available at www.ijraset.com

Weld Reinforcement Form Factor (WRFF) is the ratio of weld width to the reinforcement height. The angle between the base metal and reinforcement, which influences the fatigue strength of the weld, depends on this factor. Weld Penetration Shape Factor(WPSF) is the ratio of weld width to the penetration depth in the bead. Higher value of WPSF implies minimal reinforcement height.[4]

WRFF = Width/Reinforcement

WPSF = Width/Penetration

For constructing a structured layout to carry out the experiments, Design of Experiments (DoE) statistical techniques have been put into use and a mathematical model is obtain which is checked for competence using ANOVA technique and the results are further analysed graphically using response surface methodology (RSM). With the help of computational results, good compatibility with experimental data and effectiveness of the proposed models have been demonstrated. [5]

Stainless steel 301 is an austenitic chromium-nickel steel. High strength, exceptional corrosion resistance and weight reduction provides the ability to be widely used in multiple applications. [6] Apart from this, it possesses high ductility even when cold worked and therefore can be moulded into desired shape. Common uses of SS301 are aircraft structural parts, utensils amongst many other applications. The approximate chemistry of the material is given below in table 1.

Table 1 : Chemistry Of SS 301 (%) [7]

Mn	Si	C	Ni	N	Cr	P	S
0.790	0.620	0.100	6.850	0.057	17.000	0.027	0.003

SS301 is a variant of SS304, where Chromium-Nickel Percentage is lowered to provide high tensile strength with lower loss of ductility.[8] The electrode used of austenitic stainless steel 308-L. The electrode is consumable solid core wire of 1.2 mm diameter. The low carbon content makes the material suitable for purposes with a risk of inter-granular corrosion.[9] The chemistry is given in Table 2.

Table 2 : Chemistry of SS 308-L (%) [9]

Si	C	Mn	Nb	Ni	S	Cr	P
0.34	0.011	1.69	0.01	9.96	0.010	19.74	0.016

The investigative work aims at determining weld bead geometry and shape parameters such as reinforcement height, weld bead width and penetration during the GMA Welding. Statistical modelling has been done by developing a design matrix using Design of Experiments (DoE) and the significance of the developed model and the adequacy has been checked using ANOVA technique and results are analysed using response Surface methodology (RSM).[11,12]

II. EXPERIMENTAL SET-UP

The investigative study was carried out with the help of a welding power source of 100% duty cycle and current value ranging from 50 - 400 A, possessing a constant voltage type characteristic. The welding power source is attached to a torch which is adjusted on top of a movable carriage, the torch can be held at various angles and distances from the workpiece. The speed of the workpiece placed above the movable carriage ranges from 0 - 50 cm/min. The filler wire used was austenitic SS308L of 1.2mm diameter and was continuously fed. The machinery apparatus can be shown in Fig 2.

Fig 2 : Experimental Setup for GMAW

III. PROCEDURE FOR INVESTIGATION

A. Identifying the Input Parameters affecting the Shape and Geometry of the Bead

After extensive analysis five input parameters were found to affect the bead shape and geometry profoundly. These are Welding Speed (WS), WFR (wire feed rate), Voltage, Torch Angle (TA) and NPD (Nozzle to Plate Distance).

B. Ascertain Working Ranges of the User-Controlled Parameters

To ascertain the working ranges of all the user-controlled parameters, various trial runs were carried out, one input parameter was varied while keeping the rest at the intermediate values. The weld bead hence produced were visually observed for any defects. The working ranges were classified into 5 categories, the extreme ranges being +2 and -2, intermediate ranges were +1 and -1 whereas 0 is the central value. The ranges of the above parameters are shown in the table 3 below.

Table 3 : Working Ranges of Input Parameters

Input Parameter	Unit	LEVEL				
		-2	-1	0	+1	+2
WFR (A)	m/min	0.3	0.6	0.9	1.2	1.5
Voltage (B)	V	14	16	18	20	22
WS (C)	cm/min	70	80	90	100	110
TA (D)	Degrees	30	35	40	45	50
NPD (E)	mm	10	12.5	15	17.5	20

C. Fabrication of the Design Matrix

The design matrix shown in table 4 is constructed to establish an interrelationship between the input parameters and the response parameters.

Table 4 : Design Matrix

RUN	A (mm/min)	B (V)	C (cm/min)	D (degrees)	E (mm)	P (mm)	W (mm)	R (mm)	WRFF	WPSF
1	0	0	0	0	0	2.56	6.35	2.12	3.06	2.47
2	1	-1	1	-1	1	3.97	8.63	2.81	4.52	2.17
3	1	1	1	-1	-1	4.52	10.75	2.37	3.59	2.38
4	1	-1	-1	-1	-1	4.53	8.12	2.26	3.97	1.79
5	0	0	0	2	0	2.88	6.35	1.59	4.21	2.20
6	0	0	0	0	0	3.53	8.17	1.94	3.05	2.31
7	2	0	0	0	0	4.5	8.38	2.77	4.30	1.86
8	-1	1	-1	-1	-1	2.2	7.33	1.70	5.40	3.33
9	0	0	0	0	0	4.5	9.53	1.76	3.81	2.11
10	0	0	0	0	-2	3.2	8.07	2.11	4.05	2.52
11	0	0	-2	0	0	4.86	9.54	1.82	4.66	1.96
12	0	0	0	0	0	3.53	7.29	1.94	3.07	2.06
13	0	2	0	0	0	4.11	6.81	1.46	4.97	1.65

14	1	-1	1	1	-1	4.44	7.72	1.55	3.82	1.73
15	1	1	-1	-1	1	4.27	11.35	2.97	3.60	2.1
16	-1	-1	1	-1	-1	4.28	5.97	2.02	4.20	1.39
17	-1	-1	1	1	1	1.71	5.16	1.22	3.06	3.80
18	1	-1	-1	1	1	3.2	7.02	2.2	4.67	2.19
19	0	0	0	0	0	4.01	9.05	1.93	3.04	2.25
20	-1	-1	-1	-1	1	1.81	5.37	1.93	2.99	2.95
21	0	0	2	0	0	3.08	9.12	1.89	3.92	2.52
22	0	-2	0	0	0	4.57	7.60	1.43	5.26	1.66
23	-1	1	1	1	-1	3.52	5.63	1.07	3.90	1.59
24	0	0	0	-2	0	4.06	8	2.05	3.47	1.96
25	1	1	-1	1	-1	4.38	10.34	2.35	5.13	2.36
26	-1	1	1	-1	1	2.43	6.46	1.26	2.96	2.65
27	0	0	0	0	2	1.81	6.78	2.29	3.84	3.74
28	-1	1	-1	1	1	2.17	4.73	1.23	4.44	2.18
29	0	0	0	0	0	3.77	8.61	1.93	3.08	2.28
30	-1	-1	-1	1	-1	4.28	4.69	1.38	4.37	1.09
31	1	1	1	1	1	3.68	8.91	2.03	3.95	2.41
32	-2	0	0	0	0	1.01	3.82	0.96	3.95	3.05

D. Conducting the Experiments based on the Design Matrix

Based on the table No.4, the value of the input parameters were selected and the experiments were conducted. To avoid any methodical error the experiment was carried out in an arbitrary manner. SS301 was used with the thickness of 4mm. A section of size 50x50mm was cut and burnished. The polished section was then dipped in a solution comprising of 50g $FeCl_3$ and 120 mL HCl in 480 mL H_20. The dimensions of the bead were then calibrated.

E. Generating the Mathematical Model

The software generates second degree polynomial equation where Y is the response parameter and A,B,C,D and E are the input parameters.

Y = f (A,B,C,D,E)

The mathematical equations generated by DOE are:

1) Reinforcement = 1.93 + 0.43A - 0.01B -0.21C - 0.06D + 0.05E + 0.13AB - 0.01AC - 0.02AD + 0.13AE + 0.06BC - 0.07BD - 0.06BE - 0.06CD - 0.01CE - 0.02DE - $0.10B^2$- $0.01C^2$ + $0.08E^2$.
2) WRFF = 3.28 + 0.10A + 0.03B + 0.14C - 0.25D - 0.19E - 0.17AB + 0.10AC + 0.09AD + 0.29AE + 0.10BC - 0.23BD - 0.12BE - 0.20CD + 0.12CE + 0.13DE + $0.14A^2$ + $0.39B^2$ + $0.07C^2$ + $0.18D^2$ + $0.10E^2$.
3) WPSF = 2.27 - 0.17A + 0.07B - 0.03C + 0.05D + 0.30E + 0.05AB + 0.12AC + 0.02AD - 0.22AE - 0.15BC - 0.12BD - 0.33BE + 0.20CD + 0.17CE + 0.19DE + $0.03A^2$ - $0.16B^2$ - $0.05C^2$ - $0.01D^2$ + $0.20E^2$.
4) Penetration = 3.63 + 0.73A - 0.08B -0.12C - 0.07D - 0.48E + 0.15AB - 0.15AC - 0.07AD + 0.21AE + 0.08BC + 0.03BD + 0.29BE - 0.19CD - 0.17CE - 0.06DE - $0.20A^2$ + $0.19B^2$ - $0.02C^2$ + $0.10D^2$ - $0.26E^2$.
5) Width = 8.15 + 1.53A + 0.47B - 0.54C - 0.02D - 0.22E + 0.43AB - 0.12AD + 0.05AE - 0.17BC - 0.27BD - 0.14BE + 0.06CD - 0.13CE + 0.06DE - $0.49A^2$ - $0.21B^2$ - $0.22C^2$ + $0.31D^2$ - $0.16E^2$.

F. Testing the Adequacy of the Model.

Table 5 : ANOVA Analysis for the Developed Quadratic Models

Output parameter	F-value	P-value	R^2	Adequacy
Width	3.39	0.0209	0.8603	Adequate
Penetration	3.42	0.0201	0.8615	Adequate
Reinforcement	12.41	<0.0001	0.9576	Adequate
WRFF	3.72	0.0146	0.8712	Adequate
WPSF	10.22	0.0002	0.9489	Adequate

G. Analysis of the Achieved Results.

In this section, detailed graphical analysis has been depicted to establish a relation between the combined effect of input parameters on the response parameters.

1) Combined influence of A and E on Reinforcement

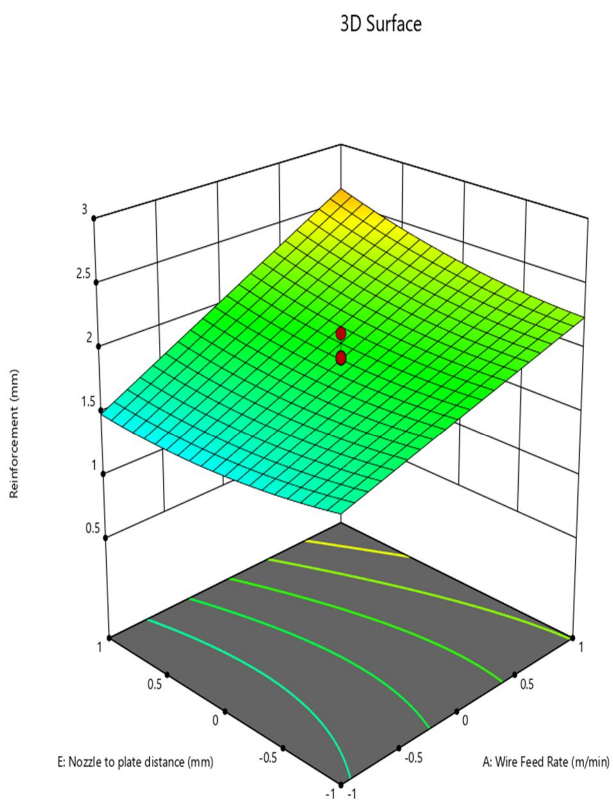

Fig 3 : Combined Influence of A and E on Reinforcement

In fig. 3, with an increase in WFR at maximum working limit of NPD, R was found to increase. It shows that WFR was found to play a more dominant role than NPD. The probable explanation to this can be the increase in the filler metal being deposited which leads to more material being deposited on the bead plate. Minimum value of reinforcement is observed at minimum values of both WFR and NPD. As NPD increases, the heat per unit length decreases leading to a decrease in reinforcement.

2) Combined effect of A and C on Reinforcement.

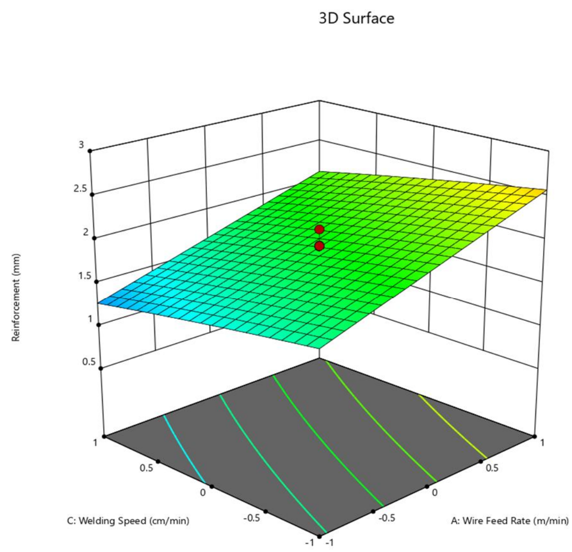

Fig 4 : Combined influence of A and C on Reinforcement

As depicted in fig. 4, maximum value of reinforcement is obtained at minimum working limit of welding speed and maximum working limit of WFR and minimum value of reinforcement is obtained at maximum welding speed and minimum WFR. This shows that increase in WFR has a positive effect on reinforcement whereas, an increase in welding speed has a negative impact on reinforcement. The possible explanation is the decrease in heat per unit length with the increase in welding speed leading to a decrease in reinforcement. On the contrary, an increase in filler metal deposition on the bead plate with the increase in WFR resulting in an increase in reinforcement.

3) Combined effect of A and B on the Width

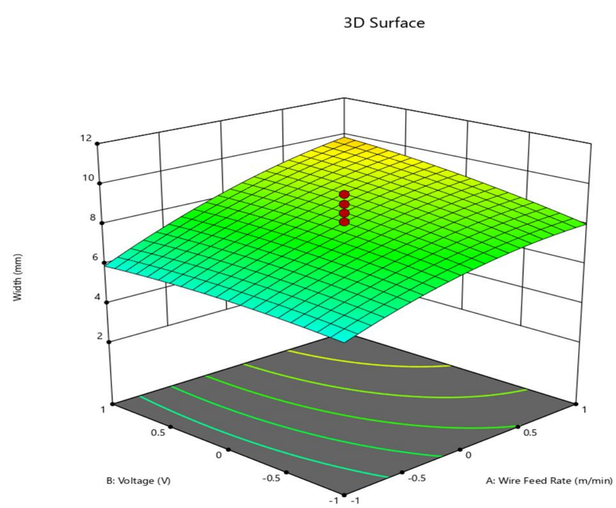

Fig 5 : Combined influence of A and B on Width

In fig 5 , width was found to increase with an increase in WFR at maximum working limit of voltage, the reason for the same is explained above in section 3.7.1. Similarly, an increase in voltage at maximum working limit of WFR leads to an increase in width, with an increase in voltage, the arc grows wider hence more area is melted around the bead leading to an increase in width.

International Journal for Research in Applied Science & Engineering Technology (IJRASET)
ISSN: 2321-9653; IC Value: 45.98; SJ Impact Factor: 7.429
Volume 8 Issue VII July 2020- Available at www.ijraset.com

4) Combined effect of A and Con Width

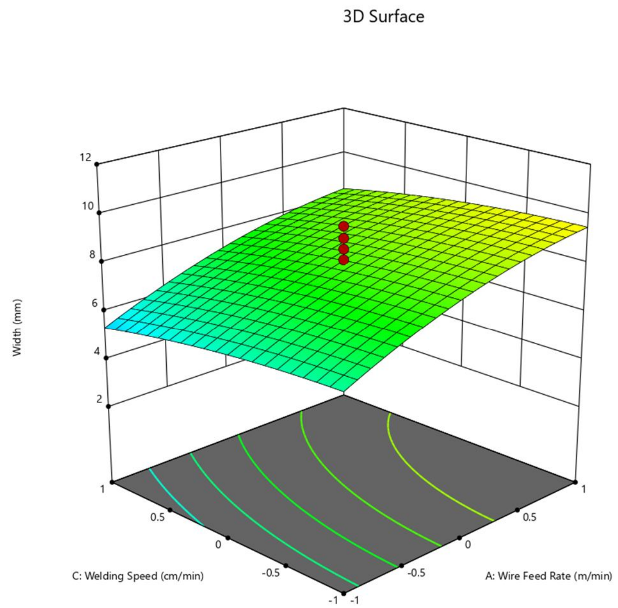

Fig 6 : Combined Influence of A and C on Width

In fig. 6, an increase in welding speed at maximum WFR results in a decrease of width, which shows that welding speed is more dominant than WFR. The probable explanation is that with the increase in welding speed, less heat is transferred per unit length as explained above in section 3.7.2.

5) Combined influence of E and A on Penetration

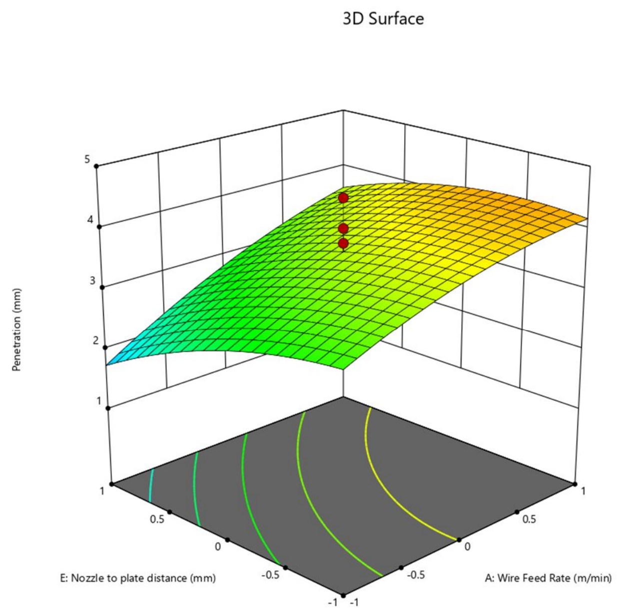

Fig 7 : Combined Influence of E and A on Reinforcement

Fig 7 illustrates that at all values of WFR, an increase in NPD results in a decrease in penetration the possible reason is with the increase in NPD, the wire before reaching the plate solidifies to a certain extent resulting in a decrease in heat input at the base plate.

6) Combined influence of C and D on Penetration.

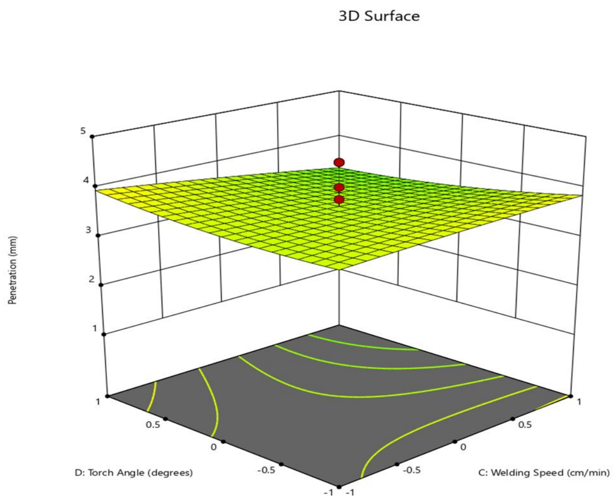

Fig 8 : Combined defect of C and D on Penetration

From fig 8, it can be inferred that at higher torch angles an increase in welding speed results in minimum penetration. The increase in either leads to a decrease in penetration since at lower torch angles the arc trails the torch pre-heating the bead plate which results in an increase in penetration whereas an opposite trend is observed at higher torch angles. Similarly, an increase in welding speed leads to a decrease in heat input and hence a decrease in penetration. At lower welding speed, with an increase in torch angle leads to a slight increase in penetration which shows that welding speed is more dominant than torch angle.

IV. INFERENCE

A. Maximum value of penetration i.e., 4.86 is obtained at minimum torch angle and central value of the rest of parameters (0,0,-2,0,0). Moreover, the minimum value i.e. 1.014, is obtained at minimum WFR (-2,0,0,0,0).

B. Maximum value of width i.e., 11.385 is obtained at (1,1,-1,-1,1) and minimum value of width is obtained at minimum WFR (-2,0,0,0,0)

C. Maximum value of reinforcement i.e., 2.97 is obtained at (1,1,-1,-1,1). Whereas, minimum reinforcement i.e., 0.967 is at (-2,0,0,0,0).

REFRENCES

[1] Murty S. S. N., Koteswara A. B., Srinivasa P., Gupta O. P., "Effect of process parameters and mathematical model for the prediction of bead geometry in pulsed GMA welding", Int. J. Adv. Manufacturing Technology (2009) 45:496–505 .

[2] Mostafa, N.B., Ph.D. Thesis on "Flux cored Arc Welding of High Strength low Alloy Steels". Department of Mechanical Engineering. IIT Delhi, India, 1992.

[3] Kwon W. H., Park C. E., Kim I. S., "Effects of Welding Process Parameters on Weld Bead Width in GMAW Processes".

[4] Kumar P., Mistry J., "Effect of Process Parameters on Bead Geometry and Shape Relationship of Gas Metal Arc Weldments".

[5] Kolahan F., Heidari M., "A New Approach for Predicting and Optimizing Weld Bead Geometry in GMAW", International Journal of Mechanical Systems Science and Engineering 2:2 2010.

[6] Eskandari, M., Najafizadeh, A., Kermanpur, A., Karimi. M., "Potential application of nanocrystalline 301 austenitic stainless steel in lightweight vehicle structures". Elsevier science Ltd., pp. 3869-3872, April-2009.

[7] Hong, T., Nagumo, M., "Effect of surface roughness on early stages of pitting corrosion of Type 301 stainless steel", Elsevier science Ltd., pp. 1665-1672, 1997.

[8] "Mathematical Modelling for prediction of Angular Distortion in MIG Welding of Stainless Steel 301" Aman Sehrawat[1], Dhruv Sharma[1], Artik[1], Pradeep Khanna[2]

[9] Technical Note, "Stainless Steel- Austenitic- 201~201L~202~204", Aalco Metals Ltd. , Parkway House, Unit 6 Parkway Industrial Estate, Pacific Avenue, Wednesbury, West Midlands, WS10 7WP.

[10] "Microstructural characterization of an SA508–309L/308L–316L domestic dissimilar metal welded safe-end joint", Hongliang Ming, Zhiming Zhang, Jianqiu Wang ⁎, En-Hou Han, Wei Ke

[11] V.Gunaraj, N.Murugan, Journal of Materials Processing Technology (1999)

[12] S.Datta, A. Bandyopadhyay, P.K. Pal, Int J Adv Manuf Technol (2008)

[13]

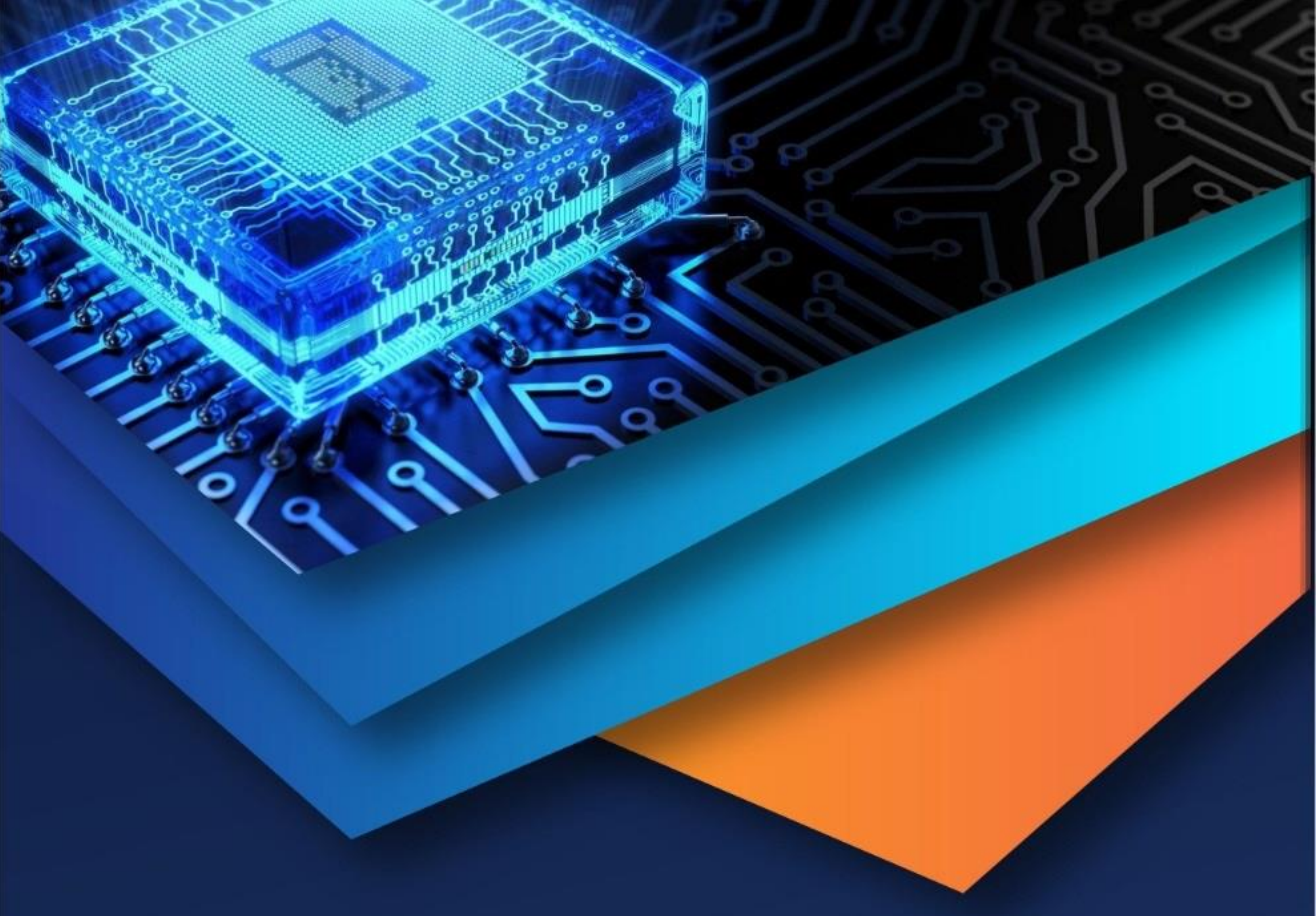

10.22214/IJRASET

INDEX COPERNICUS 45.98

IMPACT FACTOR: 7.129

IMPACT FACTOR: 7.429

INTERNATIONAL JOURNAL FOR RESEARCH

IN APPLIED SCIENCE & ENGINEERING TECHNOLOGY